phrine, metanephrine, and VMA were all within normal limits. There were also no symptoms suggesting hyperadrenocorticism and hyperserotoninemia. However, abnormally high values were noted in serum ACTH, 289 pg/ml (normal <100); serotonin, 306 ng/ml (normal <50), suggesting that the tumor produced these hormones (*6*). The serum NSE level of this patient was also high, 16.2 ng/ml (normal <10). On May 13, chest and abdominal computed tomography (CT) scans were performed. The tumor was delineated as an irregular shaped mass which involved the left hilum and posterior mediastinum ranging from 2 cm above and to 6 cm below the carina. The maximum diameter of the tumor was 6.5 cm and 7.0 cm in RL and PA directions, respectively, in the consecutive CT images. The abnormal deposit of [^{131}I]MIBG corresponded to this tumor (Fig. 1B). The abdominal CT scans revealed no metastatic foci in the abdominal cavity including the liver.

On May 15, the patient suddenly developed focal and generalized seizures. The contrast enhanced CT study performed on the next day disclosed multiple focal nodular enhancing lesions less than 1 cm in diameter in the brain suggesting brain metastases from the small cell carcinoma of the lung. He was treated with chemotherapy with VP-16 (*7*) and radiation therapy with a total dose of 40 Gy to the primary lesion. On July 3, overlapping images were again obtained 24 hr after i.v. injection of 0.5m Ci of [^{131}I]MIBG. The abnormal deposit detected in the previous chest image disappeared at this moment (Fig. 1C). This finding corresponded to that of the marked shrinkage of the tumor in the CT image taken on June 28 (Fig. 1D). No abnormal deposits of [^{131}I]MIBG were seen in the overlapping images, although brain CT scans performed on June 28 revealed slight increase in size (maximum size 2 cm in diameter) and number of the metastatic lesions. Just before and during his admission, clinical workup for detection of metastatic foci was also made by a gallium-67 tumor scan, radionuclide bone and liver scans, and abdominal echography. These diagnostic methods demonstrated no other metastatic foci. The serum levels of ACTH and serotonin measured on July 16 decreased to 92 pg/ml and 102 ng/ml, respectively.

To the best of our knowledge, this is the first case of small cell carcinoma of the lung which was delineated by [^{131}I] MIBG imaging. Iodine-131 MIBG uptake in the tumor was relatively low despite the large volume of the tumor. Therefore, much smaller brain metastatic lesions might not be visualized in the planar images. In Fig. 1A, there appears to be a focal accumulation of the tracer in the medial part of the right hepatic lobe despite no evidence of metastatis to this region. The cause of this accumulation is not clear. However, we have noticed the phenomenon that [^{131}I]MIBG in the liver decreases more rapidly in its peripheral or marginal than central portion and the tracer appears to concentrate in the region around porta hepatis with time; we therefore speculate it may represent [^{131}I]MIBG accumulation in the adrenergic neurons or bile ducts around porta hepatis. The storage sites of [^{131}I]MIBG in the tumor are not clear. We speculate that [^{131}I]MIBG may accumulate in neurosecretory granules in the cytoplasm of the tumor because it is suggested that MIBG appears to be sequestered within chromaffin granules of the adrenal medulla (*8*) and NE storage vesicles of the adrenergic nerve terminals (*9*). Further experimental and clinical studies are needed to elucidate the mechanism(s) of its uptake and retension in apudomas (*2*), and to establish the clinical role of [^{131}I]MIBG imaging in the diagnosis and management of these tumors, although [^{131}I]MIBG imaging has proven to be a reliable method for detecting pheochromocytomas (*10*).

References

1. Wieland DM, Wu JL, Brown LE, et al: Radiolabeled adrenergic neuron blocking agents: Adrenomedullary imaging with [^{131}I] iodobenzylguanidine. *J Nucl Med* 21:349–353, 1980
2. Pearse AGE, Polak JM: Endocrine tumors of neural crest origin: Neurolophomas, apudomas and the APUD concept. *Med Biol* 52:3–18, 1974
3. Moody TW, Pert CB, Gazdar AF, et al: High levels of intracellular bombesin characterize human small-cell lung carcinoma. *Science* 214:1246–1248, 1981
4. Johnson PH, Masangos PJ, Forbes JT, et al: Potential utility of serum neuron-specific enolase levels in small cell carcinoma of the lung. *Cancer Res* 44:5409–5414, 1984
5. Beierwaltes WH: Horizons in radionuclide therapy: 1985 update. *J Nucl Med* 26:421–427, 1985
6. Hori T, Nishihara H, Tateishi R, et al: Oat-cell carcinoma of the lung simultaneously producing ACTH and serotonin. *J Clin Endocrinol Metab* 37:212–219, 1973
7. Evans WK, Feld R, Osoba D, et al: VP-16 alone and in combination with cisplatin in previously treated patients with small cell lung cancer. *Cancer* 53:1461–1466, 1984
8. Wieland DM, Brown LE, Tobes MC, et al: Imaging the primate adrenal medulla with [^{123}I] and [^{131}I] metaiodobenzylguanidine: Concise communication. *J Nucl Med* 22:358–364, 1981
9. Wieland DM, Brown LE, Rogers WL, et al: Myocardial imaging with a radioiodinated norepinephrine storage analog. *J Nucl Med* 22:22–31, 1981
10. Shapiro B, Copp JE, Sisson JC, et al: Iodine-131 metaiodobenzylguanidine for the location of suspected pheochromocytoma: Experience in 400 cases. *J Nucl Med* 26:576–585, 1985

Masayuki Nakajo
Masato Taguchi
Kunisada Shimabukuro
Shinji Shinohara
Faculty of Medicine
Kagoshima University
Japan

Evolving Scintigraphic Pattern of Skeletal Metastasis from Prostatic Carcinoma

TO THE EDITOR: The most commonly encountered scintigraphic pattern in skeletal metastatic disease is multiple focal areas of increased radioactivity (*1*), while an area of photopenia or photon deficiency comprises about 3% (*2*). During progression of the disease process the scintigraphic pattern may undergo a change from one form to another (*3*). We have observed a patient with prostatic carcinoma in whom one of his skeletal metastatic foci, shown on bone scintigrams, evolved from an increased through decreased to normal tracer uptake in the lesion, and we present the case to re-emphasize that a review of previous bone scans and radiographs, including computed tomography (CT), should be a routine part of any bone scan interpretation.

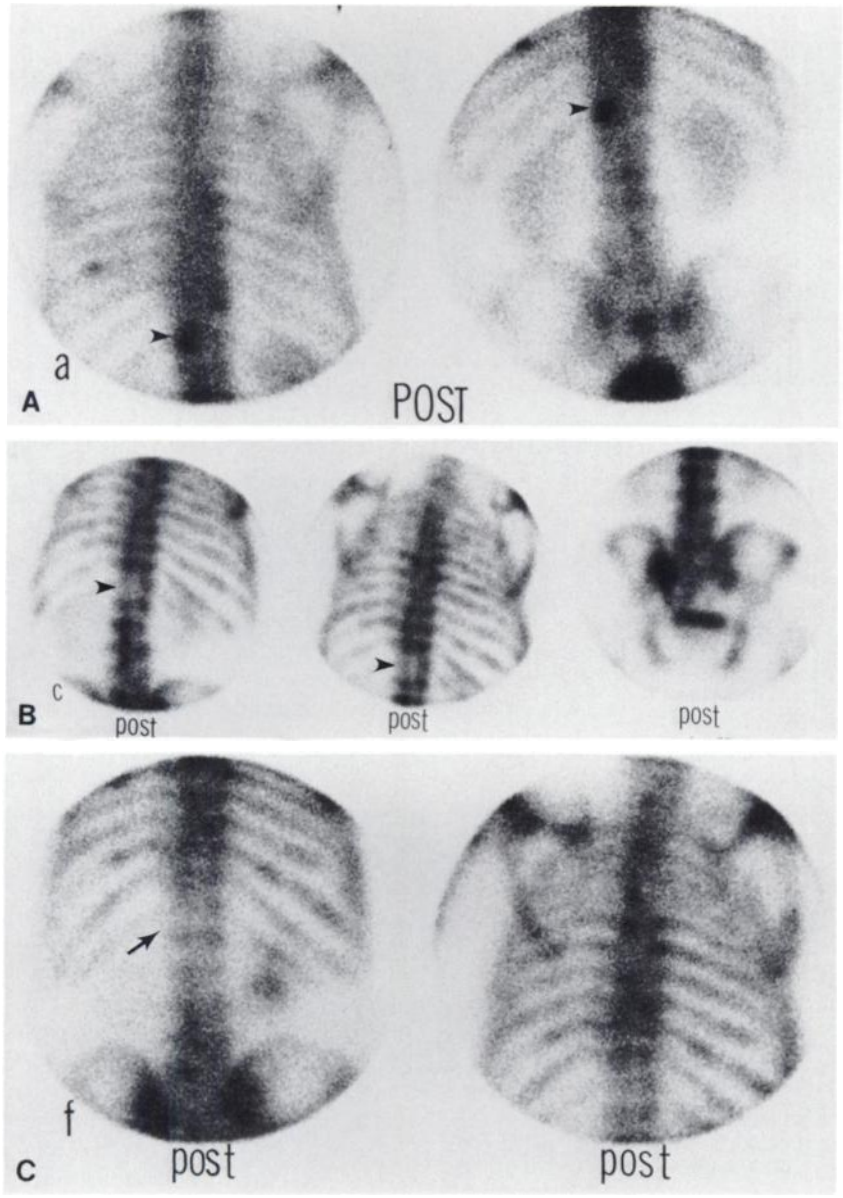

FIGURE 1
A: First bone scintigram: Focal area of increased radioactivity is seen in T-12 vertebra (arrowhead). B: Third bone scintigram performed 6 mo later. T-12 vertebral lesion was transformed to photon deficient cold area (arrowhead). C: Final bone scintigram 2.5 mo later. Almost normal appearance of lower thoracic and lumbar vertebrae (arrow) is seen

The first bone scan using technetium-99m hydroxyl methylene diphosphonate in a 76-yr-old man with prostatic carcinoma, diagnosed 3 wk previously, showed focal areas of increased radioactivity in the T-12 vertebra, the sacrum, and the left 9th rib posteriorly. There was a mild increase in radioactivity of the T-7, 8, 10, and 11 vertebrae (Fig. 1A). In spite of orchiectomy and hormonal (stilbesterol) therapy, his widespread skeletal metastases became worse as shown in a subsequent bone imaging study performed 6 mo after the second bone scintigraphy. The lesion in T-12, seen in the previous studies, became photopenic and the sacral region appeared to be normal (Fig. 1B). Another bone scintigram, performed 7 mo later demonstrated an almost normal appearing T-12 (Fig. 1C) despite the persistence of multiple lesions in other areas of the skeletal system. One week after the final bone scintigram, computed tomography (CT) of the abdomen was performed, and a lytic lesion was seen in T-12 (Fig. 2).

Thus, during a 22-mo period, sequential changes in the lesion in the T-12 vertebra on bone scan went from increased to decreased, to normal uptake of radiotracer. The manifestation of increased uptake in the lesion lasted approximately 5 mo. The photopenia in the lesion lasted 3.5 mo. The time of transition between decreased and normal uptake took 4.5 mo (total time 19.5 mo). In a previous report a change from "hot spot" to "super scan" took 20 mo (*3*).

Increased osteoblastic activity and increased regional blood flow is associated with increased tracer uptake in metastases (*1,2*). If a lesion undergoes tumor necrosis with/without therapy, in association with osteolytic activity greater than osteoblastic activity, and the lesion has a diameter over 2 cm, it will appear as a "cold area" on the bone scintigram. During progression of the disease process, whether relating to therapy or not, regeneration of bone (osteoblastic activity or lytic activity) along with improvement of the local vascularity may lead to normal appearance. A large lytic lesion was seen in the area by CT (Fig. 2). A lytic lesion seen on a radiograph may manifest as an area of increased (*2,4,5*) normal (*2,6,7*)

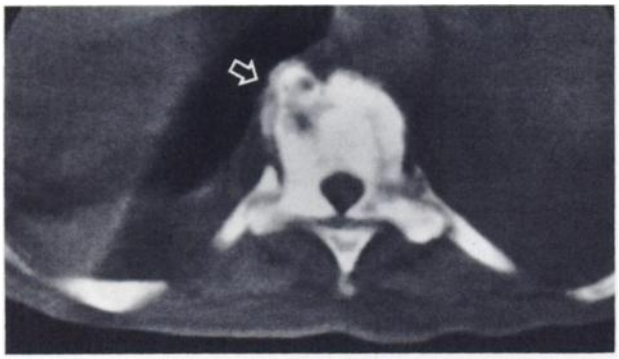

FIGURE 2
Vertebral CT concurrent with Fig. 1C. Lytic lesion is seen in T-12 (open arrow)

or decreased (*2,7,8*) activity on the bone scintigram. Imaging a lytic lesion by scintigraphy mainly depends on the size of the lytic area, the degree of reactive bone change (osteoblastic activity), and its vascularity (*2,5,7*).

While bone scintigraphy is sensitive enough to depict early skeletal metastasis, the subsequent manifestations of the scintigraphic patterns may persist as increased, or may develop to decreased or normal uptake, depending on the regional vascularity and the balance between blastic and lytic activity in the bone. To minimize false negative results during interpretation of a followup bone scintigraph, the interpreter should always review the available radiographs, including CT, in addition to concurrent comparison with previous skeletal scintigams.

References

1. Siegel BH, Alazraki NP, McNeil BJ, et al: Skeletal system. In *Nuclear Medicine Review Syllabus*, Kirchner PT, ed. New York, The Society of Nuclear Medicine, 1980, pp 555–561
2. Sy WM, Westring DW, Weinberger G: "Cold" lesions on bone imaging. *J Nucl Med* 16:1013–1016, 1975
3. Manier SM, Van Nostrand D: From "hot spots" to "super scan." *Clin Nucl Med* 8:624–625, 1983
4. Donnelly B, Johnson PM: Detection of hypertrophic pulmonary osteoarthropathy by skeletal imaging with Tc-99m labeled diphosphonate. *Radiology* 114:389–391, 1975
5. Thrall JH, Chaed N, Geslien GE, et al: Pitfalls of Tc-99m polyphosphate skeletal imaging. *AJR* 121:739–747, 1974
6. Thrupkaew WK, Jenkin RE, Quinn JL: False negative bone scans in disseminated metastatic disease. *Radiology* 113:383–386, 1974
7. Goergen TG, Alazraki NP, Halpern SE, et al: "Cold" bone lesions: A newly recognized phenomenon of bone imaging. *J Nucl Med* 15:1120–1124, 1974
8. Pendergrass HP, Potsaid MS, Castronovo FP: The clinical use of Tc-99m diphosphonate. *Radiology* 107:557–562, 1973

Wei-Jen Shih
Marguerite Purcell
Peggy A. Domstad
VA and University of Kentucky Medical Center
Lexington, Kentucky

Frank H. DeLand
Veterans Administration Medical Center
Syracuse, New York

Effect of Tumor Size on Monoclonal Antibody Uptake in Tumor Models

TO THE EDITOR: The recent paper by Hagan et al. (*J Nucl Med*, 27:422, 1986) draws attention to the effect of tumor size on the extent of monoclonal antibody uptake in experimental systems. Their data, with several different monoclonal antibodies, showed that the per gram radiopharmaceutical uptake by tumor tended to be inversely proportional to tumor size. They point out the discrepancy between those findings and ours with a radioiodine-labeled antiosteogenic sarcoma monoclonal antibody (791T/36) in a murine-human tumor system (*1*). They are, however, mistaken in the interpretation of our data with radioiodine-labeled antibody. The data, which has more recently been published elsewhere in greater detail (*2*), did not show any correlation between tumor size and the proportion of the injected dose of radioiodine/gram of tumor. Such a correlation was in fact seen between tumor weight and tumor levels of radioiodine only when the latter was expressed as a proportion of the radiolabel retained in the body. The differences between the results of these two methods of analysis was attributed to marked variation in whole-body survival of radioiodine from monoclonal antibody (*2*). This may have been due to individual differences in rate of catabolism and/or dehalogenation in tumor-bearing mice, although there was no correlation between tumor size and whole-body retention of radiolabel (*2*).

Overall, however, our studies with radioiodine-labeled antibody did show, consistently, a statistically significant proportionality between tumor size and the percent of the available dose of radiolabel (i.e., that surviving in the whole animal) which was present within tumors.

This problem of variation of whole-body survival of radioiodine-labeled 791T/36 monoclonal antibody is not seen, however, with indium-111 (^{111}In) as the radiolabel (*3*) and in view of the comments of Hagan et al. (*1*), we have now analyzed data from mice with osteosarcoma xenografts, and which had received ^{111}In-labeled 791T/36 monoclonal antibody for correlation between tumor weight and uptake of administered dose. Here mice had tumors between 0.2–0.7 g and were dissected 3 days after intraperitoneal injection of ^{111}In-791T/36 prepared as previously described (*3*). The mean whole-body survival of ^{111}In at this time was 68% ± 2.9% (s.e.m. n = 16).

Pooled data from 16 individual mice injected with ^{111}In-791T/36 is shown in Fig. 1. Tumor levels of ^{111}In expressed as a percent of the injected dose were proportional to tumor weight ($r = 0.79$, $p < 0.001$).

Overall these data, with both iodine-labeled antibody, but where tumor levels are expressed in relation to "available" radiolabel, and with ^{111}In label, where tumor levels need only be expressed in relation to dose, demonstrate that in this particular model system tumor uptake of radiolabel is proportional to tumor size. Why this differs from several other systems is unclear. A multitude of parameters can potentially affect the relationship between tumor size and antibody uptake. These include changes in blood flow, degree of necrosis,